Math Geol (2007) 39: 593–605
DOI 10.1007/s11004-007-9114-8

Forward Modeling with Forced Neural Networks for Gravity Anomaly Profile

Onur Osman · A. Muhittin Albora · Osman Nuri Ucan

Received: 9 December 2004 / Accepted: 9 December 2006 / Published online: 1 September 2007

Abstract In this paper, we introduce a new method called Forced Neural Network (FNN) to find the parameters of the object in geophysical section respect to gravity anomaly assuming the prismatic model. The aim of the geological modeling is to find the shape and location of underground structure, which cause the anomalies, in 2D cross section. At the first stage, we use one neuron to model the system and apply back propagation algorithm to find out the density difference. At the second level, quantization is applied to the density differences and mean square error of the system is computed. This process goes on until the mean square error of the system is small enough. First, we use FNN to two synthetic data, and then the Sivas–Gürün basin map in Turkey is chosen as a real data application. Anomaly values of the cross section, which is taken from the gravity anomaly map of Sivas–Gürün basin, are very close to those obtained from the proposed method.

Keywords Neural network · Gravity anomaly · Modeling · Sivas–Gürün basin

O. Osman (✉)
Istanbul Commerce University, Ragip Gumuspala Cad. No. 80, Eminonu, Istanbul, Turkey
e-mail: oosman@iticu.edu.tr

A.M. Albora
Engineering Faculty, Geophysical Department, Istanbul University, 34850, Avcilar, Istanbul, Turkey
e-mail: muhittin@istanbul.edu.tr

O.N. Ucan
Engineering Faculty, Electrical and Electronics Department, Istanbul University, 34850, Avcilar, Istanbul, Turkey
e-mail: uosman@istanbul.edu.tr

Introduction

The parameter estimation of geological structures from anomaly maps is an important subject. A classical problem in gravity and magnetic exploration is the computation of theoretical anomalies caused by idealized models of known shapes. Many researchers have published different methods for carrying out such computation, and textbooks on potential theory, e.g., Routh (2001), provide various formulas for these models. Early publications such as Barton (1929) dealt with the computation of the gradients of the gravity field. Hubbert (1948) used line-integral approach for the computation of gravitational attraction of two-dimensional masses. Bhattacharyya (1964), Nagy (1966), and Plouff (1976), presented closed form analytical solutions for prism shaped bodies, whereas Talwani and Ewing (1960), and Talwani (1965) used numerical integration techniques for the computation of the fields due to models of arbitrary shape by dividing them into polygonal prisms or laminas. Mareschal (1985) has used Fourier transform for inverse solution of gravity density distributions. Murthy et al. (1990) have focused on density differences of 2-D and 3-D gravity models. Murthy and Rao (1993a) have calculated inverse solution of gravity and magnetic anomalies of polygonal structures using Marquart algorithm. Murthy and Rao (1993b) have proposed some methods in inverse solution of gravity anomalies for circular, cylindrical, and vertical discs. Mosegaard and Tarantola (1995) have applied Monte Carlo method. Rama et al. (1999) calculated the values of depth and modified them iteratively until a best fit is achieved between the observed and calculated values.

In literature, artificial neural networks (ANN) have been applied to many scientific researches in geophysics. ANN is part of much wider field called artificial intelligence, which can be defined as the study of mental facilities through the use of computational models (Charniak and McDermott 1985). ANN is divided into two main categories: unsupervised recurrent and supervised feed-forward networks. In the unsupervised recurrent type, the networks allow information to flow in both directions. These models are called unsupervised, because there is no supervisor to set the input–output mapping relation during the learning phase. In the supervised networks, due to a set of correct input–output pairs, called the training set, the network learns the relation between the input–output pairs. ANN encompasses computer algorithms that solve classification, parameter estimation, parameter prediction, pattern recognition, completion association, filtering, and optimization problems (Brown and Poulton 1996). It has gained popularity in geophysics during the last decade, because these tools can approximate any continuous function with an arbitrary precision (Van der Baan and Jutten 2000).

The location of the buried steel drums is estimated from magnetic dipole source using supervised artificial neural network (Salem et al. 2001). Depth and radius of subsurface cavities are determined from microgravity data using back propagation neural networks (Eslam et al. 2001). Neural networks are studied to solve one and two dimensional resistivity inverse problems (El-Qady and Ushijima 2001). A new approach in neural networks, Cellular Neural Network (CNN) has been proposed by Chua and Yang (1988), which is focused on 2-D image processing. Albora et al. (2001a), and Albora et al. (2001b) applied CNN for separation of regional/residual potential sources in geophysics.

In this paper, a new forward modeling algorithm, denoted as “Forced Neural Network (FNN)” is proposed. Here, the physical parameters of buried objects are estimated by this forward modeling technique. It is applied to synthetic examples and then as a real data, Sivas–Gürün (Turkey) has been incorporated. We have found satisfactory results for both cases.

Forced Neural Network

Force Neural Network (FNN) is an information processing paradigm that is inspired by the biological neural systems, such as brain. The key element of this paradigm is the novel structure of the information processing system. It is composed of a large number of highly interconnected processing elements (neurons) working in unison to solve specific problems. FNN is configured for a specific application, such as pattern recognition or data classification, through a learning process. FNN is composed of many simple processing elements, which are massively interconnected and operate in parallel. The processing elements commonly known as neurons receive the input from previous elements and send the output to other elements through synaptic connections. These connections have different weights and to find the effective values of inputs and outputs, these values are multiplied by weights. The main purpose of neural networks is to find such weights that give the best output. Back propagation is one of the most popular learning algorithms for neural networks.

Back Propagation Algorithm

The error signal at the output of neuron j at iteration n, is defined by

$$e_j(n) = d_j(n) - y_j(n), \tag{1}$$

where neuron j is an output node, $d_j(n)$ is desired output and $y_j(n)$ is actual output of neural networks. The instantaneous value of the error energy for neuron j can be defined as $\frac{1}{2}e_j^2(n)$. Correspondingly, the instantaneous value $E(n)$ of the total error energy is obtained by summing $\frac{1}{2}e_j^2(n)$ over all neurons in the output layer; only “visible” neurons are the ones for which error signals can be calculated directly. We may thus write

$$E(n) = \frac{1}{2}\sum_{j\in C} e_j^2(n), \tag{2}$$

where the set C includes all the neurons in the output layer of the network (Haykin 1999). Let N denote the total number of patterns (examples) contained in the training set. The average squared error energy is obtained by summing $E(n)$ over all n and then normalizing with respect to set size N, as shown by

$$E_{\text{av}} = \frac{1}{N}\sum_{n=1}^{N} E(n). \tag{3}$$

The instantaneous error energy $E(n)$, and therefore the average error energy E_{av}, is a function of all the free parameters (i.e., synaptic weights and bias levels) of the network. For a given training set, E_{av} represents the cost function as a measure of learning performance. The objective of the learning process is to adjust the free parameters of the network to minimize E_{av}. To do this minimization, we use an approximation similar in rational to that used for the derivation of the Least Mean Square (LMS) algorithm.

In Forced Neural Network approach, we consider a simple method of training in which the weights are updated on a pattern-by-pattern basis until one epoch, that is, one complete presentation of the entire training set has been dealt with

$$\Delta w_{ij}(n) = \eta \delta_j(n) y_i(n), \tag{4}$$

where $\delta_j(n)$ is the local gradient and η is learning speed (Haykin 1999). Local gradient points are required changes in synaptic weights and we obtain Back-Propagation (BP) formula for the local gradient $\delta_j(n)$ as

$$\delta_j(n) = \varphi_j'\big(v_j(n)\big) \sum_k \delta_k(n) w_{kj}(n) \quad \text{neuron } j \text{ is hidden.} \tag{5}$$

Figure 1 shows the signal-flow graph representation of (5), assuming that the output layer consists of m_L neurons.

The factor $\varphi_j'(v_j(n))$ involved in the computation of the local gradient $\delta_j(n)$ in (5) depends solely on the activation function associated with hidden neuron j. The remaining factor involved in this computation, namely the summation over k, depends on two sets of terms. The first set of terms, the $\delta_k(n)$, requires knowledge of the error signals $e_k(n)$, for all neurons that lie in the layer to the immediate right of hidden neuron j, and that are directly connected to neuron j which is shown in Fig. 1. The second set of terms, the $w_{kj}(n)$, consists of the synaptic weights associated with these connections.

We may redefine the local gradient $\delta_j(n)$ for hidden neuron j as

$$\delta_j(n) = -\frac{\partial E(n)}{\partial y_j(n)} \frac{\partial y_j(n)}{\partial v_j(n)} \tag{6}$$

$$= -\frac{\partial E(n)}{\partial y_j(n)} \varphi_j'\big(v_j(n)\big) \quad \text{neuron } j \text{ is hidden.} \tag{7}$$

The local field parameter $v_j(n)$ produced at the input of the activation function associated with neuron j is therefore

$$v_j(n) = \sum_{i=0}^{m} w_{ij}(n) y_i(n), \tag{8}$$

where m is the total number of inputs (excluding the bias) applied to neuron j (e.g. Haykin 1999). The synaptic weight w_{j0} (corresponding to the fixed input $y_0 = +1$) equals the bias b_j applied to neuron$j$. Hence, the function signal $y_j(n)$ appearing at

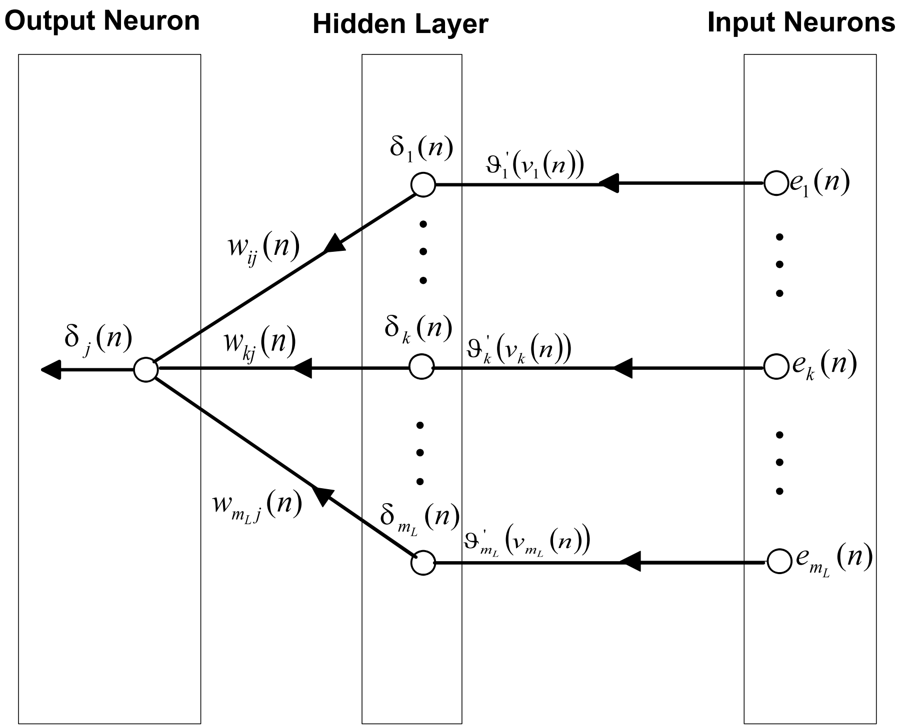

Fig. 1 Forced Neural Network (FNN) model

the output of neuron j at iteration n is

$$y_j(n) = \varphi_j\big(v_j(n)\big). \tag{9}$$

Next differentiating (9) with respect to $v_j(n)$, we get

$$\frac{\partial y_j(n)}{\partial v_j(n)} = \varphi_j'\big(v_j(n)\big), \tag{10}$$

where the use of prime (the right-hand side) signifies differentiation with respect to the argument (Haykin 1999).

Forced Neural Network Application for Gravity Anomaly

This technique could be used to model any type of body geometrics and density contrasts. We begin with a prismatic structure, and the gravity anomaly function at point z because of any prismatic unit located at (x, h) coordinates can be given as

$$A(z, x, h) = 2 \times 6.67 \times 10^{-8} \times \Delta\rho$$

$$
\begin{aligned}
&\times \Bigg\{ (x \times wdt - z \times wdt) \\
&\times \ln\left(\sqrt{\frac{(h \times dpt + dpt)^2 + (x \times wdt - z \times wdt)^2}{(h \times dpt)^2 + (x \times wdt - z \times wdt)^2}}\right) \\
&- \big((x \times wdt - z \times wdt) - wdt\big) \\
&\times \ln\left(\sqrt{\frac{(h \times dpt + dpt)^2 + ((x \times wdt - z \times wdt) - wdt)^2}{(h \times dpt)^2 + ((x \times wdt - z \times wdt) - wdt)^2}}\right) \\
&+ (h \times dpt + dpt) \arctan\left(\frac{x \times wdt - z \times wdt}{h \times dpt + dpt}\right) \\
&- \arctan\left(\frac{x \times wdt - z \times wdt - wdt}{h \times dpt + dpt}\right) \\
&- h \times dpt \arctan\left(\frac{x \times wdt - z \times wdt}{h \times dpt}\right) \\
&- \arctan\left(\frac{x \times wdt - z \times wdt - wdt}{h \times dpt}\right) \Bigg\}.
\end{aligned} \tag{11}
$$

$\Delta\rho$ is density difference, wdt and dpt are width and depth of each prismatic unit, x and h are the locations of each prismatic units in cross-section. $A(z, x, h)$ can also be shown as below by extracting $\Delta\rho$ from (11).

$$A(z, x, h) = \Delta\rho \times A_r(z, x, h) \tag{12}$$

$A(z)$ can be calculated as taking the summations of (11) over all h and x locations.

$$A(z) = \sum_{x=0}^{n_c-1} \sum_{h=0}^{n_r-1} A(z, x, h). \tag{13}$$

There are n_r rows and n_c columns. Thus, cross-section can be represented as $n_r \times n_c$ prismatic units with a known depth and length.

In our method, weights of the neuron are assigned as $\Delta\rho_{i,j}$ for each pixel and activation function has a linear property such as the outputs are the same as the inputs. After using the back propagation, $\Delta\rho_{i,j}$ are updated and the output of the neuron gives the gravity anomaly. Hence, the density differences are found. But, the results of this system are not sufficient because non-uniqueness and horizontal locations are constrained therefore, the value of $\Delta\rho$ is set to zero if its value is very close to the zero according to the density difference which is obtained from geological features of the region, otherwise the value of $\Delta\rho$ is set to the density difference of the geological region after back propagation.

Forced neural network means that after sufficient epoch is applied, fixed values are assigned to the output of the neuron according to the density difference $\Delta\rho$, and this

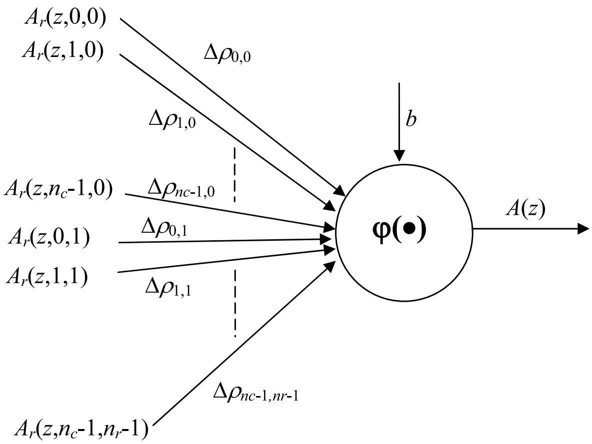

Fig. 2 Application of Forced Neural Network (FNN) for gravity anomaly maps

process is continued until the mean square error of the output, $A(z)$ which is shown in Fig. 2, becomes sufficiently small.

Performance of the Algorithm in Synthetic Data

In geophysics, Forced Neural Networks (FNN) method is applied to synthetic prismatic structures. In these examples, density contrasts are chosen as $\Delta\rho = 1\ \mathrm{g/cm}^3$. We used two-dimensional forward modeling equations of (e.g. Talwani and Ewing 1960) and then obtained gravity anomaly of synthetic underground structure. First of all, the anomaly of synthetic data is concerned, then, shape, location, and density difference parameters of the buried structure are estimated using forward modeling technique, FNN.

In our first example, the underground model upper depth is 450 m, and lower depth is 650 m. The width of the upper part is 100 m, while lower part is 350 m as shown in Fig. 3. The anomalies of this model are considered as input data of FNN. In synthetic examples, every learning cycle is comprised of 345 epochs and two-level quantization ($\Delta\rho$ or zero) is applied for each 10 learning cycle, which is found experimentally. The estimated geological structure obtained after the FNN application, results in similar anomaly profile (dashed line) as the observed anomaly (solid line) shown in Fig. 3.

For our second synthetic model, we have chosen another prismatic structure. The estimated geological structure obtained after FNN application results in similar anomaly profile (dashed line) as the observed anomaly (solid line) shown in Fig. 4. In both examples, satisfactory results are obtained.

Example of Application on Real Data

As an application field, anomaly map placed at the Northwest side of the mine ore in Sivas–Gürün in Turkey is chosen (Fig. 5). The underground structure is a basin,

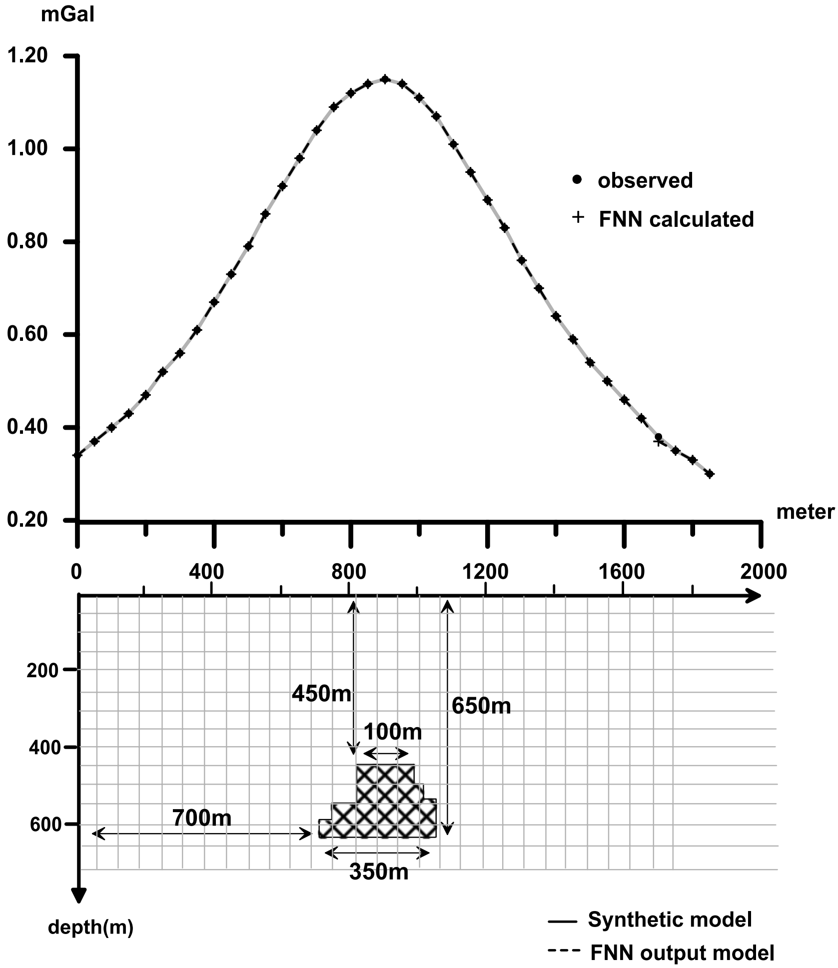

Fig. 3 First synthetic forward model. FNN output is shown by *dashed line* and observed anomaly is shown by *solid line*

which has $-0.5\ \mathrm{g/cm}^3$ density difference according to the crystallized limestone. At the end of the studies on this field, it is found out that the oldest units are the limestone, the age of Upper Cretaceous Cenomanien. Upper side of this part, Conglomerate at the age of Neogene, red clay and sandstone are placed as a discordant. The region has faults with direction of NE-SW (Dogan et al. 1989; Albora 1992).

After two synthetic examples, we study the Bouguer anomaly map of Sivas basin, which is shown in Fig. 6. Anomalies are measured in every 50 m and the average $\Delta\rho$ is found as $-0.5\ \mathrm{g/cm}^3$ after various optimization steps using (11). Low pass filter with a 0.02 cutoff frequency is applied to the anomaly map and this residual anomaly map is shown in Fig. 7. Profile A1–A2 in residual anomaly map is considered for modeling with FNN algorithm. The width of the units is 50 m. To find more precise

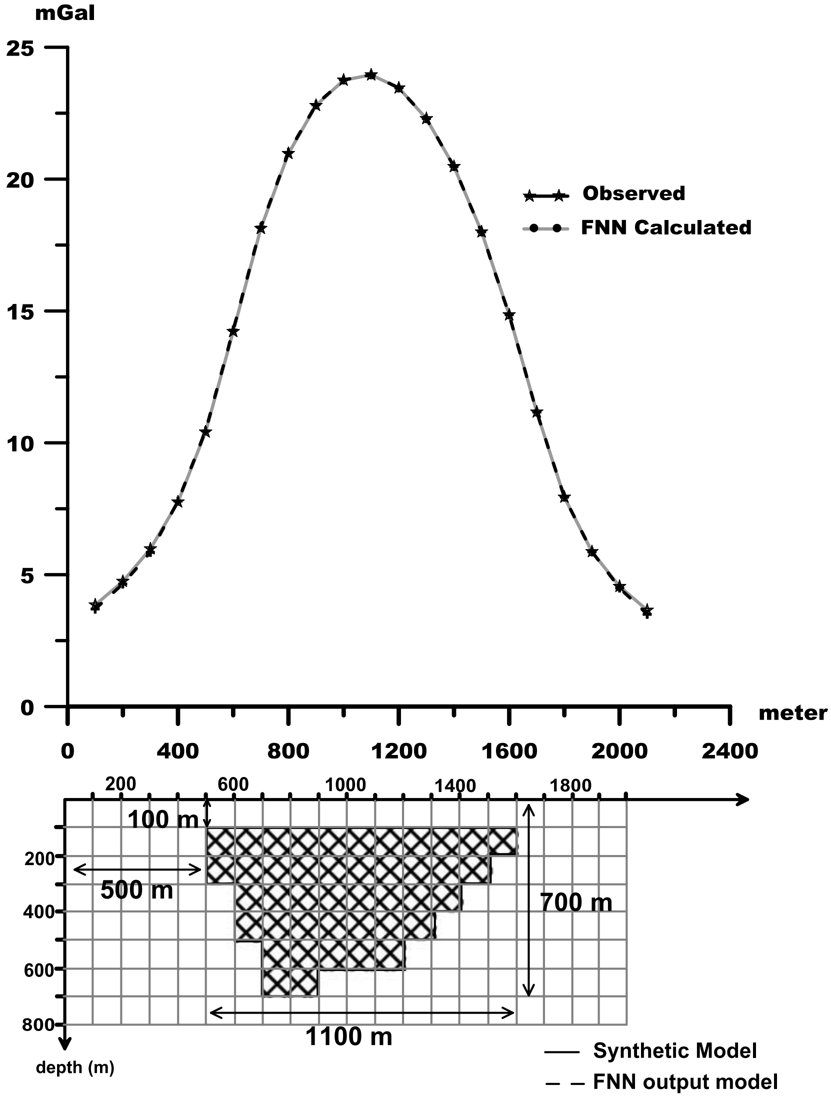

Fig. 4 Second synthetic forward model. FNN output is shown by *dashed line* and observed anomaly is shown by *solid line*

results by FNN algorithm, the depth of each unit is taken as 25 m. At the end of the optimization, the model in Fig. 8 is reached with its estimated and observed anomaly curves. The anomaly of our model and the original anomaly are very close to each other. Mean square error of the anomaly of our model is only 0.0579 and it fits the original one.

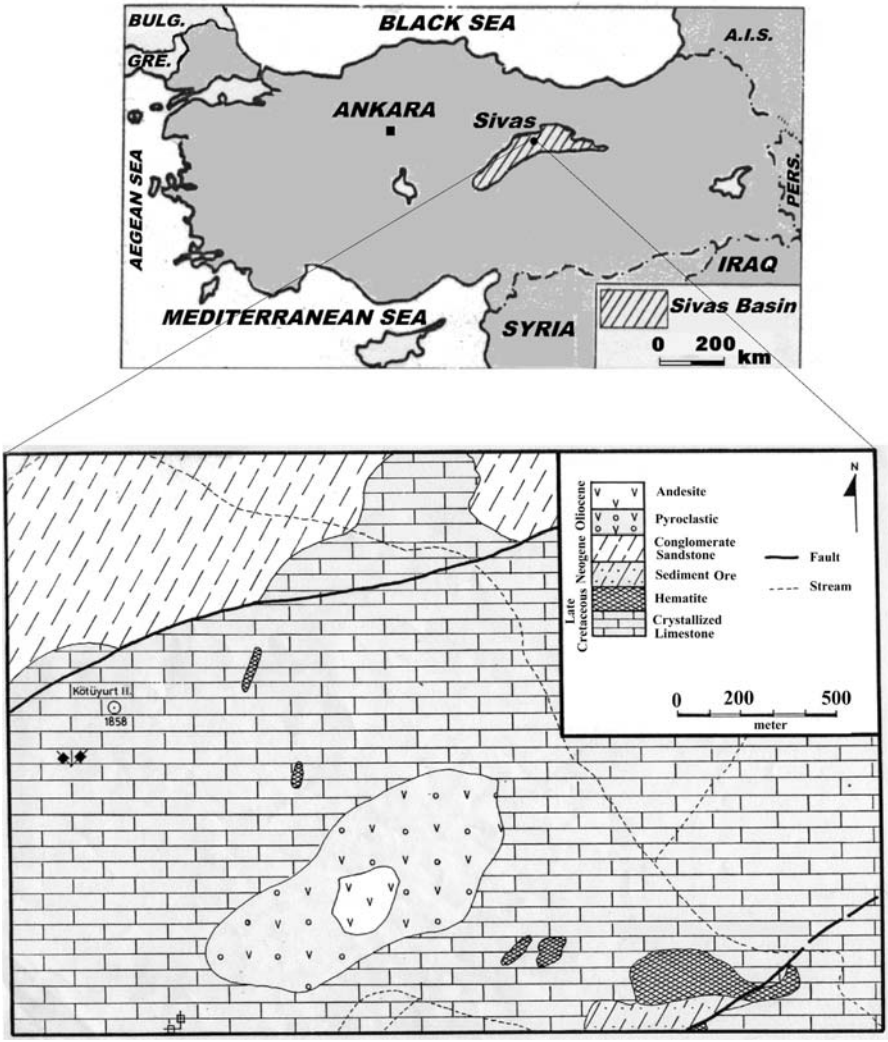

Fig. 5 Modified geology map of our working region (MTA Reports, Dogan et al. 1989)

Conclusions

The Forced Neural Networks (FNN) presented in this paper clearly shows that the gravity field at any point due to a solid body with uniform volume density can be computed as the field due to a fictitious distribution of surface mass-density on the same body. First of all, we applied the FNN technique to two synthetic data. In synthetic examples, two prisms are chosen. In both cases, FNN outputs match the mathematically obtained gravity anomalies. There is only a small error at the peek of the anomalies. As a real data application, gravity anomaly of carsick basin near Sivas–Gürün in Turkey is considered. The average difference of density in the field

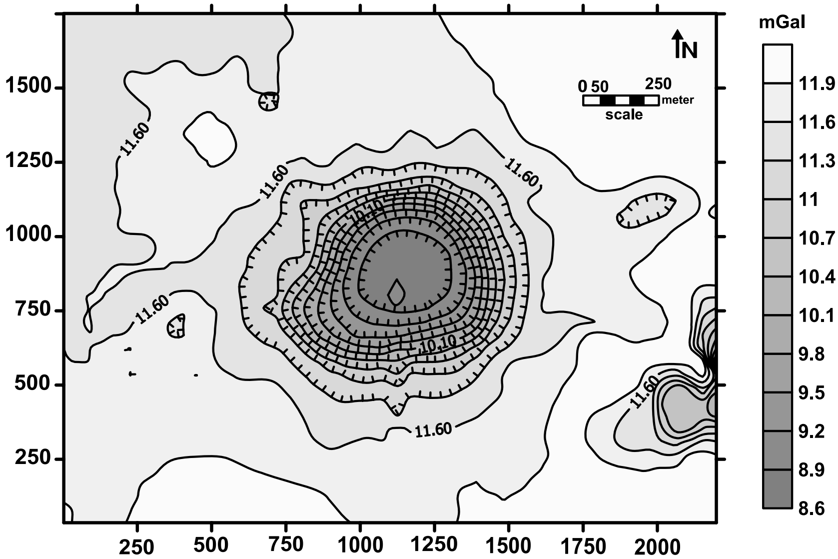

Fig. 6 Bouguer anomaly map of Sivas–Turkey (interval contour is 0.3 mGal)

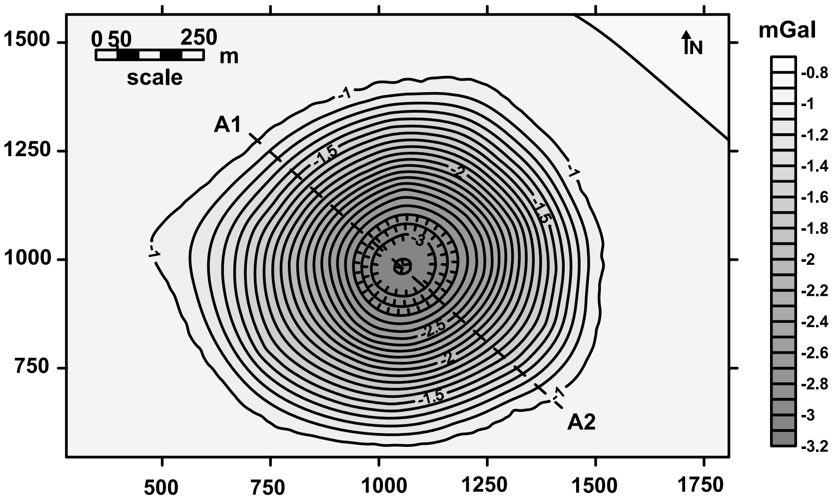

Fig. 7 Residual anomaly map (interval contour is 0.1 mGal)

is computed as $-0.5\ \text{g/cm}^3$. Cross-section, which is taken from A1–A2 profile in Fig. 7 residual anomaly map, is indicated with a solid line in Fig. 7. The anomaly of the model, which is created by FNN, is shown in Fig. 8 with dotted line. Both two anomalies fit satisfactorily. This modeling technique is so powerful that it can be applied to any type of structure without any prior information. Thus, we estimate the parameters of underground model using FNN approach. The width of our estimated structure is 550 m, upper depth is 50 m, and lower depth is 325 m as seen in Fig. 8.

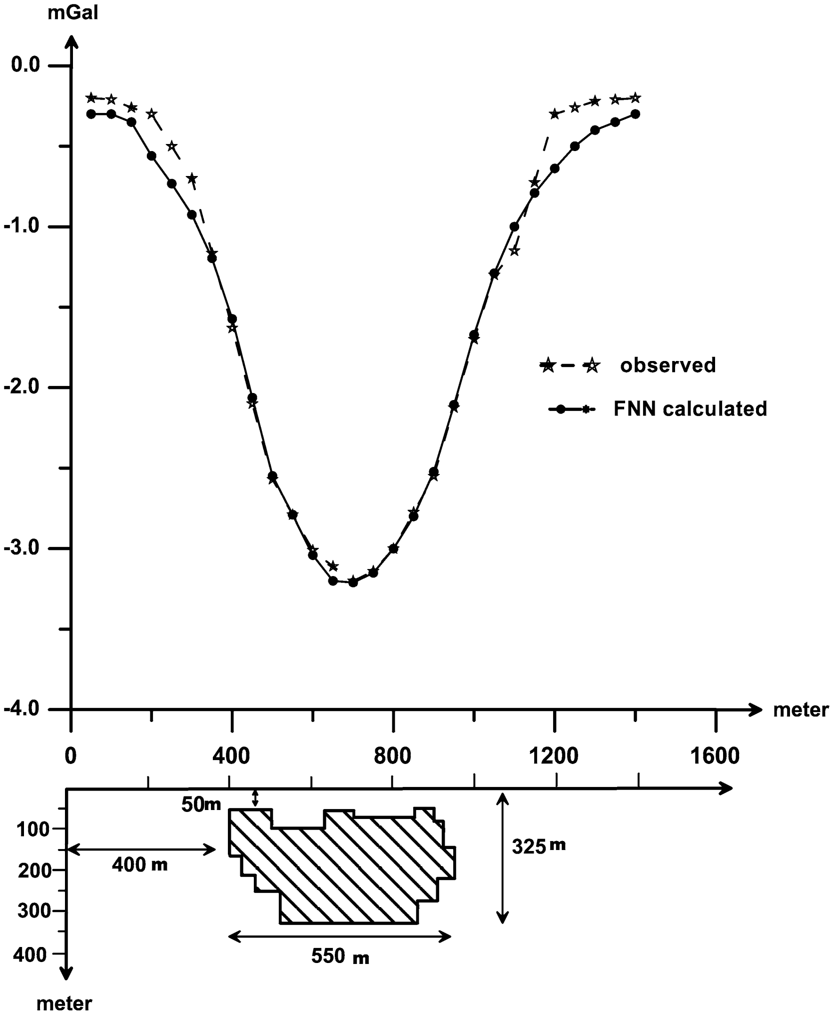

Fig. 8 Observed anomaly of the cross-section is shown with (⋆) signs and the anomaly of FNN model is shown with (•) signs. Geological model, which is calculated by FNN method, is given with *hatched field* in the cross-section (width and depth of each unit are 50 and 25 meters respectively and $\Delta\rho = -0.5\ \mathrm{g/cm^3}$)

Acknowledgements This work was supported by the Research Fund of the University of Istanbul. Project Numbers: 1247/050599 and 28/03092002.

References

Albora AM (1992) Study of gravity effect of different geometrical structure with monograms. M.Sc. thesis, Institute of Science Technology, Indiana University, USA, 49p

Albora AM, Ucan ON, Ozmen A (2001a) Residual separation of magnetic fields using a cellular neural network approach. Pure Appl Geophys 158:1797–1818

Albora AM, Ucan ON, Ozmen A, Ozkan T (2001b) Evaluation of Sivas-Divrigi region Akdag iron ore deposits using cellular neural network. J Appl Geophys 46:129–142

Barton DC (1929) Calculations in the interpretation of observations with the Eötvös torsion balance. AIME 1:481–486
Bhattacharyya BK (1964) Magnetic anomalies due to prism-shaped bodies with arbitrary polarization. Geophysics 29:517–531
Brown MP, Poulton MM (1996) Location buried objects for environmental site investigations using neural networks. J Environ Eng Geophys 1:179–188
Charniak E, McDermott D (1985) Introduction to artificial intelligence. Addison-Wesley, Reading, 701p
Chua LO, Yang L (1988) Cellular neural networks: Theory. IEEE Trans Circuits Syst 35:1257–1272
Dogan H, Yildizeli N, Yurt MZ, Celebi A, Ozcen H (1989) Geological iron ore report 89/120 on Sivas Divrigi and its environment with project number AR: 33613-Poligon-II. IR: 922 and with the support of TDCI General Management (MTA report), 89/120 Ankara, p 35
El-Qady G, Ushijima K (2001) Inversion of Dc resistivity data using neural networks. Geophys Prospect 49:417–430
Eslam E, Salem A, Ushijima K (2001) Detection of cavities and tunnels from gravity data using a neural network. Explor Geophys 32:204–208
Haykin S (1999) Neural networks. Prentice Hall, New York, 852p
Hubbert MK (1948) A line integral method of computing the gravimetric effects of two-dimensional masses. Geophysics 13:215–225
Mareschal JC (1985) Inversion of potential field data in Fourier transform domain. Geophysics 50:685–691
Mosegaard K, Tarantola A (1995) Monte Carlo sampling of solutions to inverse problems. J Geophys Res 100:431–447
Murthy IVM, Rao PR, Rao SJ (1990) The density difference and generalized programs for two and three-dimensional gravity modeling. Comput Geosci 16:277–287
Murthy IVR, Rao PR (1993a) Inversion of gravity and magnetic anomalies of two-dimensional polygonal cross sections. Comput Geosci 19:1213–1228
Murthy IVR, Rao SJ (1993b) Gravity inversion of horizontal circular discs and vertical circular cylinders. Comput Geosci 20:821–838
Nagy D (1966) Gravitational attraction of a right rectangular prism. Geophysics 31:362–371
Plouff D (1976) Gravity and magnetic fields of polygonal prisms and application to magnetic terrain corrections. Geophysics 41:727–741
Rama Rao P, Swamy KV, Radhakrishna Murty IV (1999) Inversion of gravity anomalies of three-dimensional density interfaces. Comput Geosci 25:887–896
Routh EJ (2001) In: A treatise on analytical statistics with numerous examples, vol. II. Elibron, p 280–296
Salem A, Ravat D, Johnson R, Ushijima K (2001) Detection of buried steel drums from magnetic anomaly data using a supervised neural network. J Environ Eng Geophys 6:115–122
Talwani M, Ewing M (1960) Rapid computation of gravitational attraction of 3D bodies of arbitrary shape. Geophysics 25:203–225
Talwani M (1965) Computation with the help of a digital computer of magnetic anomalies caused by bodies of arbitrary shape. Geophysics 30:797–817
Van der Baan M, Jutten C (2000) Neural networks in geophysics. Geophysics 65:1032–1047